arXiv:1206.0969v2 [hep-lat] 28 Jul 2012

Phase structure for lattice fermions with flavored chemical potential terms

Tatsuhiro Misumi*

Physics Department, Brookhaven National Laboratory, Upton, NY 11973, USA

We discuss the chiral phase diagram in the parameter space of lattice QCD with minimal-doubling fermions, which can be seen as lattice fermions with flavored chemical potential terms. We study strong-coupling lattice QCD with the Karsten-Wilczek formulation, which has one relevant parameter μ_3 as well as gauge coupling and a mass parameter. We find a nontrivial chiral phase structure with a second-order phase transition between chiral symmetric and broken phases. To capture the whole structure of the phase diagram, we study the related lattice Gross-Neveu model. The result indicates that the chiral phase transition also exists in the weak-coupling region. From these results we speculate on the μ_3-g^2 chiral phase diagram in lattice QCD with minimal-doubling fermions, and discuss their application to numerical simulations.

---

*Electronic address: tmisumi@bnl.gov

I. INTRODUCTION

The famous no-go theorem [1, 2] states that lattice fermion actions with chiral symmetry, locality and other common features must produce massless degrees of freedom in multiples of two in a continuum limit. This is contradictory with a phenomenological fact that there exist only three quarks with masses below the QCD scale. By now several fermion constructions to bypass the no-go theorem have been developed, although all of them have their individual shortcomings: The explicit chiral symmetry breaking with the Wilson fermion approach [3] results in an additive mass renormalization, which in turn requires a fine-tuning of the mass parameter for QCD simulations. Domain-wall [4, 5] and overlap fermions [6, 7] produce a single fermion mode by modifying the definition of chiral symmetry or introducing the momentum-dependent chiral charge, although they lead to rather expensive simulations algorithms.. These approaches attempt to realize single fermionic degrees of freedom by breaking the requisite conditions for the no-go theorem. On the other hand, there is another direction to approach numerical simulations. According to [1], Hypercubic symmetry and reflection positivity of actions result in 2^d species of fermions where d stands for the dimension. Thus it is potentially possible to reduce the number of species by breaking hypercubic symmetry properly. Actually, the staggered fermion approach [8–12], with only 4 species of fermions does this and possesses flavored-hypercubic symmetry instead. However this requires rooting procedures for the physical 2 or $(2+1)$-flavor QCD simulation.

A possible goal in this direction is a lattice fermion with 2 species, the minimal number required by the no-go theorem. Such a minimal-doubling action was first proposed by Karsten, and later by Wilczek [13, 14]. Other than the original type, two more types are known as Creutz-Borici type [15–17] and Twisted-ordering type [18]. These fermions all possess one exact chiral symmetry and ultra locality. As such they could be faster for simulation, at least for two-flavor QCD, than other chirally symmetric lattice fermions. However it has been shown [19–22] that we need to fine-tune several parameters for a continuum limit with these actions. This is because they lack sufficient discrete symmetry to prohibit redundant operators from being generated through loop corrections [23–26]. Thus the minimally doubled fermions have not been extensively used so far. Nevertheless, there is the possibility to apply them to simulations if one can efficiently perform the necessary fine-tuning of parameters.

In this paper we pursue the chiral phase structure in the parameter plane for minimal-doubling lattice QCD for two purposes: One purpose is to understand properties of these formulations theoretically. The other purpose is to show their applicability to lattice QCD simulations since understanding a nontrivial phase diagram, as with the Aoki phase in Wilson fermion [27–31], can be useful in showing the applicability to lattice QCD. We first show that minimal-doubling fermions can be seen as a special case of lattice fermions with species-dependent (imaginary) chemical potential terms. We focus on the Karsten-Wilczek formulation with one relevant parameter μ_3, which corresponds to a mass parameter in the analogy of Wilson fermion. We next investigate the chiral phase structure in the space of the gauge coupling and this relevant parameter. We analyze strong-coupling lattice QCD, and show that chiral symmetry is spontaneously broken in a certain range of the parameter while the chiral condensate is zero outside the range. We find a second-order phase transition between these chiral symmetric and broken phases. We also show that pion becomes massless as a Nambu-Goldstone boson in the chiral-broken phase while the sigma meson becomes massless on the second-order phase boundary due to the critical behavior of the second-order phase transition. We investigate the lattice Gross-Neveu model to capture an entire phase structure. From these results we suppose a similar chiral phase structure in 4d QCD with flavored-chemical-potential lattice fermions, and discuss their applicability to lattice QCD simulations.

In Sec. II, we study lattice fermions with flavored chemical potential, or minimal-doubling fermions. In Sec. III, we investigate a chiral phase structure in the framework of strong-coupling lattice QCD. In Sec. IV, we study the Gross-Neveu model to obtain information of the whole phase diagram. In Sec. V, we discuss a phase structure in 4d QCD from the results of the last two sections. Section VI is devoted to a summary and discussion.

II. FLAVORED-CHEMICAL-POTENTIAL FERMION

In this section we study minimal-doubling fermions and their generalization. Before going to the main theme, let us remind ourselves of Wilson's prescription to shirk the no-go theorem. Wilson fermion extracts one light fermion by introducing a species-dependent mass term, which we call a "flavored-mass term". A free action and a Dirac operator of Wilson fermion are given by

$$S_{\rm W} \,=\, a^4\sum_{n,\mu}\bar{\psi}_n\gamma_\mu\frac{\psi_{n+\mu}-\psi_{n-\mu}}{2a}+a^5\sum_{n,\mu}\bar{\psi}_n\frac{2\psi_n-\psi_{n+\mu}-\psi_{n-\mu}}{2a^2}, \tag{1}$$

$$aD_{\rm W}(p)=i\gamma_\mu\sin p_\mu a\,+\,\sum_\mu(1-\cos p_\mu a). \tag{2}$$

We here exhibits a lattice spacing a to manifest mass dimensions of each term. In this formulation, 15 out of 16 species have $O(1/a)$ mass and are decoupled in the naive continuum limit. As shown in [32], this is not the only case of flavored-mass terms. There are four types of nontrivial flavored-mass terms ($M_{\rm f}=M_{\rm P}$, $M_{\rm V}$, $M_{\rm A}$, $M_{\rm T}$), which satisfy γ_5 hermiticity and give second-derivative terms up to $O(a^2)$ errors as with the usual Wilson term. A general form of Wilson-type fermions are written as

$$aD_{\rm fm}(p)=i\gamma_\mu\sin p_\mu a\,+M_{\rm f}(p), \tag{3}$$

where $M_{\rm f}(p)$ stands for flavored-mass terms. Details of species-splitting depends on explicit forms of $M_{\rm f}(p)$ [32].

We now consider further deformation of the fermion action. We multiply $M_{\rm f}$ by γ_4 or $i\gamma_4$ as

$$aD_{\rm fc}(p)=i\gamma_\mu\sin p_\mu a\,+(i)\gamma_4M_{\rm f}(p). \tag{4}$$

In these cases, degeneracy of species is lifted by specie-dependent real or imaginary chemical potential terms, not by species-dependent mass. It means that we can get rid of some doublers by this method too. We name such terms as “flavored-chemical-potential terms”, and name lattice fermions with them as “flavored-chemical-potential (FCP) fermions”. (We will later discuss problems with this kind of naive introduction of chemical potential [37].) It is obvious that a real type of FCP terms breaks down γ_5 hermiticity and leads to a sign problem while an imaginary type keeps it and has no sign problem. An outstanding point in this formulation is that ultra-locality and one exact $U(1)$ chiral symmetry remains intact as

$$\{\gamma_5,D_{\rm fc}(p)\}=0. \tag{5}$$

(See Refs. [32–36] for details of chiral symmetry in this type of lattice fermions.) In principle, by using this deformation we can reduce 16 species to smaller multiple numbers of two without losing all chiral symmetries. We note that the chemical potential term, of course,

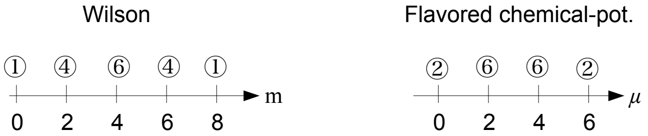

FIG. 1: Species-splitting in Wilson and Karsten-Wilczek fermion. Circled numbers stand for the number of massless flavors on each point.

breaks hypercubic symmetry into cubic symmetry and breaks C, P, T into CT and P [19–22] as far as $M_f(p)$ is cubic-symmetric. It means that this formulation automatically corresponds to finite-density systems unless we tune several parameters. In this paper we concentrate on the following explicit form of imaginary-type FCP fermions,

$$S_{\mathrm{KW}} = a^4 \sum_{n,\mu} \bar{\psi}_n \gamma_\mu \frac{\psi_{n+\mu} - \psi_{n-\mu}}{2a} + a^5 \sum_{j=1}^{3} \bar{\psi}_n i\gamma_4 \frac{2\psi_n - \psi_{n+j} - \psi_{n-j}}{2a^2}, \tag{6}$$

$$aD_{\mathrm{KW}}(p) = i\gamma_\mu \sin p_\mu a \, + \, i\gamma_4 \sum_{j=1}^{3} (1 - \cos p_j a). \tag{7}$$

Here 14 species is decoupled in the naive continuum limit while two species at $p = (0, 0, 0, 0)$ and $p = (0, 0, 0, \pi/a)$ has zero mass and zero imaginary chemical potential [52]. More precisely, among 16 species, two species have zero imaginary chemical potential, six have $2/a$, six have $4/a$ and two have $6/a$. In Fig. 1 we compares specie-splitting of KW fermion in chemical potential space to that of Wilson fermion in mass space. It is notable that two-flavor is the minimal number allowed by the no-go theorem. This form has been known as the Karsten-Wilczek (KW) fermion [13, 14], which is the first known type of "minimal-doubling fermions" [13–18]. It has one exact chiral symmetry, ultra-locality, cubic symmetry, CT and P. Since the chemical potential term breaks discrete symmetries into the subgroup, we need to fine-tune three parameters for one dimension-3 ($\bar{\psi} i\gamma_4 \psi$) and two dimension-4

($\bar{\psi}\gamma_4\partial_4\psi,\ F_{j4}F_{j4}$) counterterms in order to take a Lorentz-symmetric continuum limit for the zero-(T,μ) lattice QCD simulations [24–26].

Among the three counterterms, in this paper we mainly deal with the dimension-3 term $\mu_3\bar{\psi}i\gamma_4\psi$ with a relevant parameter μ_3 and the dimension-4 term $d_4\bar{\psi}\gamma_4\partial_4\psi$ with a marginal parameter d_4 since we study the strong-coupling lattice QCD and the Gross-Neveu model, which contain no plaquette action. In particular the parameter μ_3 is of special importance: It changes the number of flavors and plays an important role in the chiral phase structure. Furthermore the quantum effects produce $O(1/a)$ additive chemical potential renormalization in this case instead the additive mass renormalization, and we need to cancel it by adjusting μ_3 even for the application to the imaginary-chemical-potential lattice QCD. This necessity of parameter tuning is also understood from the well-known fact that the naive introduction of chemical potential into lattice fermions leads to divergence of energy density and requires a counterterm due to the violation of the abelian gauge invariance as shown in Ref. [37].

We here write the KW fermion action of the interacting theory as

$$\begin{aligned}
S_{\mathrm{KW}} \;=\; \sum_n \Bigg[& \frac{1}{2}\sum_{\mu=1}^{4} \bar{\psi}_n\gamma_\mu \left(U_{n,n+\mu}\psi_{n+\mu} - U_{n,n-\mu}\psi_{n-\mu}\right) \\
& + \frac{r}{2}\sum_{j=1}^{3} \bar{\psi}_n i\gamma_4 \left(2\psi_n - U_{n,n+j}\psi_{n+j} - U_{n,n-j}\psi_{n-j}\right) + \mu_3\bar{\psi}_n i\gamma_4\psi_n + m\bar{\psi}_n\psi_n \\
& + \frac{d_4}{2}\bar{\psi}_x\gamma_4 \left(U_{n,n+4}\psi_{n+4} - U_{n,n-4}\psi_{n-4}\right) \Bigg],
\end{aligned} \tag{8}$$

where we introduce a parameter r in analogy with the Wilson parameter. We introduce the dimension-3 counterterm with the parameter μ_3. Although we mainly focus on μ_3 in this work, we also introduce the dimension-4 counterterm with the parameter d_4 in Eq. (8) which is also relevant for the strong-coupling study. We make all the quantities dimensionless. Now let us look into how the number of flavors depend on μ_3. For a free theory, the associated massless Dirac operator in momentum space is

$$aD_{\mathrm{KW}}(p) = i\sum_{\mu=1}^{4}\gamma_\mu \sin ap_\mu + i\gamma_4(\mu_3 + 3r - r\sum_{j=1}^{3}\cos ap_j + d_4\sin ap_4). \tag{9}$$

We first look into a minimal-doubling range for μ_3 and the speed of light in the range. We for simplicity take $r=1$. For $-1-d_4 < \mu_3 < 1+d_4$, we have only two zeros, both of which have the form as $\bar{p}=(0,0,0,\frac{1}{a}\arcsin(-\frac{\mu_3}{1+d_4}))$. By expanding the momentum as $p=\bar{p}+q$ around the zeros, the coefficient of $i\gamma_4$ in the Dirac operator is given as

$$\begin{aligned}(1+d_4)[\sin a\bar{p}_4\cdot\cos aq_4+\cos a\bar{p}_4\cdot\sin aq_4]+\mu_3+3-\sum_{i=1}^{3}\cos(\bar{p}_i+q_i)\\ =[(1+d_4)\cos a\bar{p}_4]\,aq_4+O(a^2q^2).\end{aligned}\tag{10}$$

Therefore, for general values of μ_3 in this range, the speed of light is modified as

$$\sim q_4(1+d_4)\sqrt{1-\frac{\mu_3^2}{(1+d_4)^2}}+O(aq^2).\tag{11}$$

We can fix this speed of light to a correct value up to the $O(a)$ discretization errors by taking $(1+d_4)^2=1+\mu_3^2$. We will discuss details of Lorentz symmetry restoration in Sec.V. Now, let us classify μ_3 parameter regions by the number of physical flavors in the free theory. Since d_4 just gives a shift of the parameter regions, we now consider $d_4=0$ for simplicity. The above minimal-doubling range is given just by $-1<\mu_3<1$. For $-7<\mu_3<-5$, we again have two zeros. For $\mu_3<-7$ and $\mu_3>1$, there is no zero of the Dirac operator, which means that there are no physical fermions. For $-5<\mu_3<-3$ and $-3<\mu_3<-1$, six zeros exist. $\mu_3=1,-7$ have one zero, but the dispersion relations have a unphysical form as $\sim\mathbf{p}+p_4^2$. $\mu_3=-1,-5$ have four zeros, but the dispersions are unphysical. $\mu_3=-3$ has six zeros, but the dispersion is again unphysical. In the end, the parameter ranges where physical fermions can be described are $-7<\mu_3<-5$ (2 flavors), $-5<\mu_3<-3$ (6 flavors), $-3<\mu_3<-1$ (6 flavors), $-1<\mu_3<1$ (2 flavors). We summarize it in Fig. 2. We note that nonzero d_4 gives larger minimal-doubling range as shown above.

What we want to study in this work is how these parameter ranges evolve in the finite gauge coupling direction. The most important question for practical use of this formulation in lattice QCD is how the two-flavor range, or the minimal-doubling range changes in the interacting theory. Our question is deeply related to a possible chiral phase structure with respect to the $U(1)$ chiral symmetry. It is because spontaneous chiral symmetry breaking is expected to occur only in parameter ranges with physical fermions. We thus speculate that boundaries between χSSB and non-χSSB phases starts from $\mu_3=-7$ and $\mu_3=1$ in the weak-coupling limit. From next section, we will elucidate the μ_3-g^2 chiral phase diagram by using strong-coupling lattice QCD and the Gross-Neveu model.

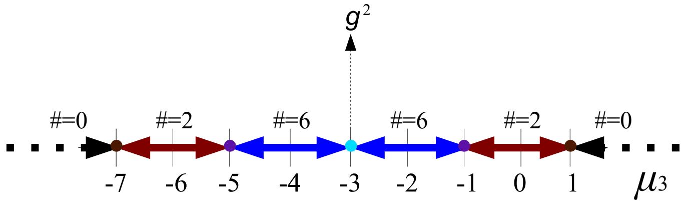

FIG. 2: The number of species in Karsten-Wilczek fermion as a function of the parameter μ_3. On the boundaries between different sectors, the dispersion relation of fermions becomes unphysical.

III. STRONG-COUPLING LATTICE QCD

In this section we employ the strong coupling analysis to investigate the chiral phase structure in lattice QCD with Karsten-Wilczek (KW) fermion. The first step is to derive an effective potential of meson fields corresponding to the fermion action in Eq. (8). The strong-coupling study for KW fermion was first performed by the present author and collaborators in [38]. We here take the same approach.

Lattice fermion action is generally written as following by using hopping operators $P_\mu^\pm$ and an onsite operator $\hat{M}$

$$S = \sum_{n,\mu} \bar{\psi}_n (P_\mu^+ \psi_{n+\mu} - P_\mu^- \psi_{n-\mu}) + \sum_n \bar{\psi}_n \hat{M} \psi_n. \tag{12}$$

By using these operators an effective action for mesons in the strong coupling limit can be written [8] as

$$\begin{aligned} S_{\text{eff}}(\mathcal{M}) &= N_c \sum_n \left[\sum_\mu \mathrm{Tr}\, f(\Lambda_{n,\mu}) + \mathrm{tr}\, \hat{M}\mathcal{M}(n) - \mathrm{tr}\ \log \mathcal{M}(\mathrm{n}) \right], \qquad (13) \\ \Lambda_{n,\mu} &= \frac{V_{n,\mu}\bar{V}_{n,\mu}}{N_c^2}, \quad \mathcal{M}(n)^{\alpha\beta} = \frac{\sum_a \bar{\psi}_n^{a,\alpha}\psi_n^{a,\beta}}{N_c}, \end{aligned}$$

$$V_{n,\mu}^{ab} = \bar{\psi}_n^b P_\mu^- \psi_{n+\hat{\mu}}^a\,, \quad \bar{V}_{n,\mu}^{ab} = -\bar{\psi}_{n+\hat{\mu}}^b P_\mu^+ \psi_n^a\,, \tag{14}$$

$$\mathrm{Tr}\, f(\Lambda_{n,\mu}) = -\mathrm{tr}\, f\left(-\mathcal{M}(n)(P_\mu^+)^{\mathrm{T}}\mathcal{M}(n+\hat{\mu})(P_\mu^-)^{\mathrm{T}}\right)\,, \tag{15}$$

where N_c is the number of colors, Tr (tr) means a trace over color(spinor) index, and $\mathcal{M}(n)$ is a meson field. a, b are indices for colors while α, β for spinors. The explicit form of the function f is determined by performing a one-link integral of the gauge field. In the large N_c limit, it is known that $f(x)$ can be analytically evaluated [10] as

$$f(x) = \sqrt{1+4x} - 1 - \ln\frac{1+\sqrt{1+4x}}{2} = x + O(x^2)\,. \tag{16}$$

For most cases of studying phase structure, we can approximate it as $f(x) \sim x$, which corresponds to a large-dimension limit [39]. Since the phase transition is expected to be second-order for a massless case, this approximation at least works well near the phase boundary. We however note that it becomes less valid for large σ. In the case of the Karsten-Wilczek fermion, we have $\hat{M} = m\mathbf{1}_4 + \mathrm{i}(\mu_3 + 3r)\gamma_4^{\mathrm{T}}$ and

$$P_\mu^+ \;=\; \begin{cases} \frac{1}{2}(\gamma_\mu + ir\gamma_4) & \mu = 1,2,3 \\ \frac{1}{2}\gamma_4(1+d_4) & \mu = 4 \end{cases}, \quad P_\mu^- \;=\; \begin{cases} \frac{1}{2}(\gamma_\mu - ir\gamma_4) & \mu = 1,2,3 \\ \frac{1}{2}\gamma_4(1+d_4) & \mu = 4 \end{cases}. \tag{17}$$

We here assume a form of meson condensate with chiral and 4th vector condensates as

$$\mathcal{M}_0 = \sigma\mathbf{1}_4 + i\pi_4\gamma_4. \tag{18}$$

It is because the flavored chemical potential term is expected to produce 4th vector condensate, which is related to quark density. (We will discuss possibility of other condensates in the end of this section.) The explicit form of the effective action for σ and π_4 is given by

$$S_{\text{eff}} = -4N_c \mathrm{Vol.}\mathcal{V}_{\text{eff}}(\sigma, \pi_4), \tag{19}$$

$$\begin{aligned} \mathcal{V}_{\text{eff}}(\sigma, \pi_4) = {} & \frac{1}{2}\log(\sigma^2 + \pi_4^2) - m\sigma + (\mu_3 + 3r)\pi_4 \\ & - \frac{1}{4}[3(1+r^2) + (1+d_4)^2]\sigma^2 - \frac{1}{4}[3(1-r^2) - (1+d_4)^2]\pi_4^2. \end{aligned} \tag{20}$$

We now find saddle points of $S_{\text{eff}}(\mathcal{M})$ from

$$\frac{\delta S_{\text{eff}}}{\delta\sigma} = \frac{\delta S_{\text{eff}}}{\delta\pi_4} = 0. \tag{21}$$

Then gap equations are given by

$$\frac{3(1+r^2) + (1+d_4)^2}{2}\sigma + m - \frac{\sigma}{\sigma^2 + \pi_4^2} \;=\; 0\,, \tag{22}$$

$$\frac{3(1-r^2) - (1+d_4)^2}{2}\pi_4 - (\mu_3 + 3r) - \frac{\pi_4}{\sigma^2 + \pi_4^2} \;=\; 0\,. \tag{23}$$

It is notable that these gap equations have a particle-hole symmetry as $(\pi_4, \mu_3 + 3) \leftrightarrow (-\pi_4, -\mu_3 - 3)$, which is reflected by chiral phase structure as we will see later. We first consider $m = 0$, and solve the equations analytically. One of the main purposes here is to find a boundary between chiral symmetric and broken phases. For this purpose we take $\sigma = 0$ after dividing the first equation by σ since σ is an order parameter of chiral symmetry breaking. Then we have

$$\frac{3(1+r^2)+(1+d_4)^2}{2} = \frac{1}{\pi_4^2}\,, \tag{24}$$

$$\frac{3(1-r^2)-(1+d_4)^2}{2}\pi_4 - (\mu_3 + 3r) = \frac{1}{\pi_4}\,. \tag{25}$$

These equations give chiral boundaries for μ_3 as

$$\mu_3 = \pm\frac{6r^2+2(1+d_4)^2}{\sqrt{6r^2+2(1+d_4)^2+6}} - 3r. \tag{26}$$

Therefore we have two ranges of μ_3 with different chiral properties, **I** and **II** :

$$\mathbf{I}: \quad \mu_3 < -\frac{6r^2+2(1+d_4)^2}{\sqrt{6r^2+2(1+d_4)^2+6}} - 3r, \qquad \mu_3 > \frac{6r^2+2(1+d_4)^2}{\sqrt{6r^2+2(1+d_4)^2+6}} - 3r, \tag{27}$$

$$\mathbf{II}: \quad -\frac{6r^2+2(1+d_4)^2}{\sqrt{6r^2+2(1+d_4)^2+6}} - 3r < \mu_3 < \frac{6r^2+2(1+d_4)^2}{\sqrt{6r^2+2(1+d_4)^2+6}} - 3r. \tag{28}$$

The question is which corresponds to the chiral symmetric or broken phases. We for a while look into the $r = 1$ case to show details of chiral phase structure. Since the change of d_4 just shift the chiral phase boundary (26), we for a while take $d_4 = 0$ to catch the chiral phase structure although we note that we need to take care of it for a Lorentz symmetric continuum limit. For $r = 1$ and $d_4 = 0$ the boundaries are given by $\bar{\mu}_3 \equiv \mu_3 + 3 = \pm\sqrt{32/7}$ ($\mu_3 \sim -5.14, -0.86$). Here we defined shifted μ_3 as $\bar{\mu}_3 = \mu_3 + 3$. By solving the gap equations in Eq. (8)(23) for $r = 1$ and $d_4 = 0$ we derive two solutions of chiral and π_4 condensates as

$$\mathcal{M}_0^A: \quad \sigma = 0, \quad \pi_4 = -\bar{\mu}_3 + \sqrt{\bar{\mu}_3^2 - 2}, \tag{29}$$

and

$$\mathcal{M}_0^B: \quad \sigma = \frac{\sqrt{32-7\bar{\mu}_3^2}}{4\sqrt{7}}, \quad \pi_4 = -\frac{\bar{\mu}_3}{4}. \tag{30}$$

By comparing effective potentials of the two solutions, we find which corresponds to vacua for the two parameter ranges, **I** and **II**. We show the following by substituting the two solutions: $\mathcal{V}_{\text{eff}}(\mathcal{M}_0^A) - \mathcal{V}_{\text{eff}}(\mathcal{M}_0^B) > 0$ for $-\sqrt{32/7} < \bar{\mu}_3 < \sqrt{32/7}$ (**II**) while $\mathcal{V}_{\text{eff}}(\mathcal{M}_0^A) - \mathcal{V}_{\text{eff}}(\mathcal{M}_0^B) < 0$

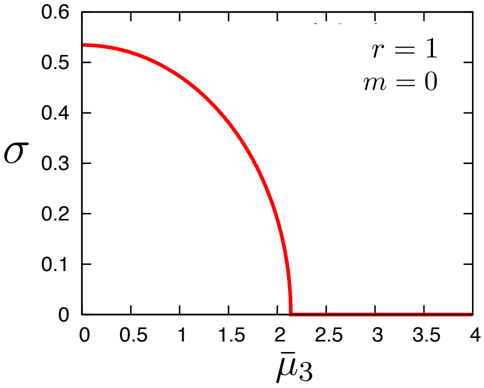

FIG. 3: Chiral condensate in strong-coupling lattice QCD with KW fermion for $m = 0$ and $r = 1$. We define $\bar{\mu}_3 \equiv \mu_3 + 3$ and depict the chiral condensate as a function of $\bar{\mu}_3$ for $0 < \bar{\mu}_3 < 4$. This result indicates the second-order chiral transition although the approximation $f(x) \sim x$ becomes less reliable for larger σ.

for $\bar{\mu}_3 < -\sqrt{32/7}$, $\bar{\mu}_3 > \sqrt{32/7}$ (**I**). To sum up, the chiral symmetric and broken phases are given by

$$\sigma = 0 \qquad \text{for} \quad \mu_3 < -\sqrt{32/7} - 3,\ \mu_3 > \sqrt{32/7} - 3 \ \ (\mathbf{I}), \tag{31}$$

$$\sigma = \frac{\sqrt{32 - 7(\mu_3 + 3)^2}}{4\sqrt{7}} \quad \text{for} \quad -\sqrt{32/7} - 3 < \mu_3 < \sqrt{32/7} - 3 \ \ (\mathbf{II}). \tag{32}$$

The behavior of chiral condensate is depicted as a function of $\bar{\mu}_3 = \mu_3 + 3$ in Fig. 3, which shows that the transition between chiral symmetric and broken phases is second-order. We also depict parameter regions for the two phases in the strong-coupling limit for $r = 1$, $d_4 = 0$ and $m = 0$ in Fig. 4. As seen from Eq. (26), a nonzero d_4 gives a larger physical range (**II**) with SSB of chiral symmetry.

We show that the order of transition becomes a crossover for $m \neq 0$. Fig.5 shows the chiral condensate as a function of $\bar{\mu}_3 = \mu_3 + 3$ and m. It is obvious that the second-order phase transition changes into a crossover for $m \neq 0$. We note that π_4 condensate is in general non-zero in the chiral-broken phase. π_4 becomes zero only for $\mu_3 + 3 = 0$, which corresponds to a theory with unphysical dispersions.

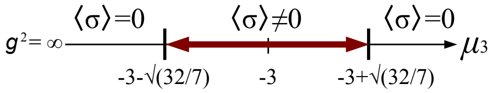

FIG. 4: Chiral phase structure in the strong-coupling limit of lattice QCD with KW fermion for $r = 1$, $d_4 = 0$ and $m = 0$.

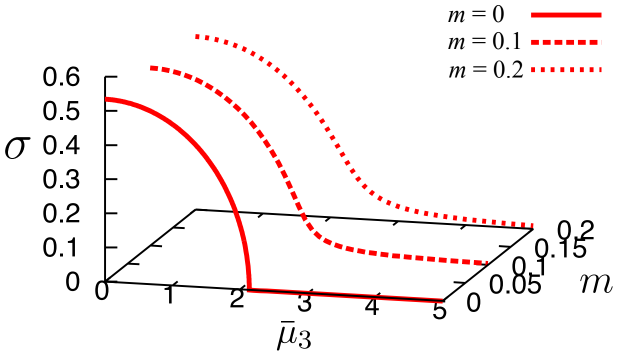

FIG. 5: Chiral condensate in strong-coupling lattice QCD with KW fermion for $r = 1$ and $d_4 = 0$ as a function of $\bar{\mu}_3$ and m.

We next look into mass of mesons within the same framework. We here consider $m = 0$ but general values of r and d_4. To calculate meson masses we expand the meson field as,

$$\mathcal{M}(n) = \mathcal{M}_0^{\mathrm{T}} + \sum_X \pi^X(n)\Gamma_X^{\mathrm{T}}\,, \quad X \in \{S, P, V_\alpha, A_\alpha, T_{\alpha\beta}\}\ , \tag{33}$$

where S, P, V_α, A_α and $T_{\alpha\beta}$ stand for scalar, pseudo-scalar, vector, axial-vector and tensor respectively. Here $\mathcal{M}_0$ is the vacuum expectation value of $\mathcal{M}(n)$. We note that

$$\Gamma_S = \frac{\mathbf{1}_4}{2},\ \Gamma_P = \frac{\gamma_5}{2},\ \Gamma_{V_\alpha} = \frac{\gamma_\alpha}{2},\ \Gamma_{A_\alpha} = \frac{i\gamma_5\gamma_\alpha}{2},\ \Gamma_{T_{\alpha\beta}} = \frac{\gamma_\alpha\gamma_\beta}{2i}\ (\alpha < \beta). \tag{34}$$

Then the effective action at the second order of π^X is given by

$$\begin{aligned} S_{\text{eff}}^{(2)} &= N_c \sum_n \left[\frac{1}{2} \mathrm{tr}\,(\mathcal{M}_0^{-1}\Gamma_X \mathcal{M}_0^{-1}\Gamma_Y)\,\pi^X(n)\pi^Y(n) + \sum_\mu \mathrm{tr}\,(\Gamma_X P_\mu^- \Gamma_Y P_\mu^+)\pi^X(n)\pi^Y(n+\hat{\mu}) \right] \\ &= N_c \int \frac{d^4p}{(2\pi)^4} \pi^X(-p) D_{XY}(p) \pi^Y(p)\,, \end{aligned} \tag{35}$$

where

$$D_{XY}(p) = \frac{1}{2}\big(\widetilde{D}_{XY}(p) + \widetilde{D}_{YX}(-p)\big), \tag{36}$$

$$\widetilde{D}_{XY}(p) = \frac{1}{2}\mathrm{tr}\,(\mathcal{M}_0^{-1}\Gamma_X \mathcal{M}_0^{-1}\Gamma_Y) + \sum_\mu \mathrm{tr}\,(\Gamma_X P_\mu^- \Gamma_Y P_\mu^+) e^{ip_\mu}. \tag{37}$$

In our case $\mathcal{M}_0 = \sigma\mathbf{1} + i\pi_4\gamma_4$ gives

$$\mathcal{M}_0^{-1} = \frac{1}{\sigma^2 + \pi_4^2}(\sigma\mathbf{1} - i\pi_4\gamma_4). \tag{38}$$

We now write the whole inverse meson propagator matrix in the S-V-T-A-P sector as

$$D_{SVTAP} =$$

$$\left[\begin{array}{cccccccccccccccc}
D_S & -C & \frac{-irs_1}{2} & \frac{-irs_2}{2} & \frac{-irs_3}{2} & & & & & & & & & & & \\
-C & D_{V_4} & & & & & & & & & & & & & & \\
\frac{irs_1}{2} & & D_{T_{14}} & & & & & & & & & & & & & \\
\frac{irs_2}{2} & & & D_{T_{24}} & & & & & & & & & & & & \\
\frac{irs_3}{2} & & & & D_{T_{34}} & & & & & & & & & & & \\
 & & & & & D_{V_3} & & & & & & \frac{-irs_2}{2} & \frac{irs_1}{2} & & & \\
 & & & & & & D_{V_2} & & & & & \frac{irs_3}{2} & & \frac{-irs_1}{2} & & \\
 & & & & & & & D_{V_1} & & & & & \frac{-irs_3}{2} & \frac{irs_2}{2} & & \\
 & & & & & & & & D_{T_{12}} & & & & & C & \frac{-irs_3}{2} & \\
 & & & & & & & & & D_{T_{13}} & & & -C & & \frac{irs_2}{2} & \\
 & & & & & & & & & & D_{T_{23}} & C & & & \frac{-irs_1}{2} & \\
 & & & & & \frac{irs_2}{2} & \frac{-irs_3}{2} & & & & C & D_{A_1} & & & & \\
 & & & & & \frac{-irs_1}{2} & & \frac{irs_3}{2} & & -C & & & D_{A_2} & & & \\
 & & & & & & \frac{irs_1}{2} & \frac{-irs_2}{2} & C & & & & & D_{A_3} & & \\
 & & & & & & & & \frac{irs_3}{2} & \frac{-irs_2}{2} & \frac{irs_1}{2} & & & & D_P & \\
 & & & & & & & & & & & & & & & D_{A_4}
\end{array}\right], \tag{39}$$

where components are given by

$$D_S = \frac{\sigma^2 - \pi_4^2}{2(\sigma^2+\pi_4^2)^2} + \frac{1}{4}[(1+r^2)(c_1+c_2+c_3) + (1+d_4)^2 c_4], \tag{40}$$

$$D_{V_4} = \frac{\sigma^2 - \pi_4^2}{2(\sigma^2+\pi_4^2)^2} - \frac{1}{4}[(1-r^2)(c_1+c_2+c_3) - (1+d_4)^2 c_4], \tag{41}$$

$$D_{V_3} = \frac{1}{2(\sigma^2+\pi_4^2)} - \frac{1}{4}[(1+r^2)(c_1+c_2) + (r^2-1)c_3 + (1+d_4)^2 c_4], \tag{42}$$

$$D_{V_2} = \frac{1}{2(\sigma^2+\pi_4^2)} - \frac{1}{4}[(1+r^2)(c_1+c_3) + (r^2-1)c_2 + (1+d_4)^2 c_4], \tag{43}$$

$$D_{V_1} = \frac{1}{2(\sigma^2+\pi_4^2)} - \frac{1}{4}[(1+r^2)(c_2+c_3) + (r^2-1)c_1 + (1+d_4)^2 c_4], \tag{44}$$

$$D_{T_{14}} = \frac{1}{2(\sigma^2+\pi_4^2)} - \frac{1}{4}[(r^2-1)(c_2+c_3) + (1+r^2)c_1 + (1+d_4)^2 c_4], \tag{45}$$

$$D_{T_{24}} = \frac{1}{2(\sigma^2+\pi_4^2)} - \frac{1}{4}[(r^2-1)(c_1+c_3) + (1+r^2)c_2 + (1+d_4)^2 c_4], \tag{46}$$

$$D_{T_{34}} = \frac{1}{2(\sigma^2+\pi_4^2)} - \frac{1}{4}[(r^2-1)(c_1+c_2) + (1+r^2)c_3 + (1+d_4)^2 c_4], \tag{47}$$

$$D_{T_{12}} = \frac{\sigma^2 - \pi_4^2}{2(\sigma^2+\pi_4^2)^2} + \frac{1}{4}[(r^2-1)(c_1+c_2) + (1+r^2)c_3 + (1+d_4)^2 c_4], \tag{48}$$

$$D_{T_{13}} = \frac{\sigma^2 - \pi_4^2}{2(\sigma^2+\pi_4^2)^2} + \frac{1}{4}[(r^2-1)(c_1+c_3) + (1+r^2)c_2 + (1+d_4)^2 c_4], \tag{49}$$

$$D_{T_{23}} = \frac{\sigma^2 - \pi_4^2}{2(\sigma^2+\pi_4^2)^2} + \frac{1}{4}[(r^2-1)(c_2+c_3) + (1+r^2)c_1 + (1+d_4)^2 c_4], \tag{50}$$

$$D_{A_1} = \frac{\sigma^2 - \pi_4^2}{2(\sigma^2+\pi_4^2)^2} + \frac{1}{4}[(1+r^2)(c_2+c_3) + (r^2-1)c_1 + (1+d_4)^2 c_4], \tag{51}$$

$$D_{A_2} = \frac{\sigma^2 - \pi_4^2}{2(\sigma^2+\pi_4^2)^2} + \frac{1}{4}[(1+r^2)(c_1+c_3) + (r^2-1)c_2 + (1+d_4)^2 c_4], \tag{52}$$

$$D_{A_3} = \frac{\sigma^2 - \pi_4^2}{2(\sigma^2+\pi_4^2)^2} + \frac{1}{4}[(1+r^2)(c_1+c_2) + (r^2-1)c_3 + (1+d_4)^2 c_4], \tag{53}$$

$$D_{A_4} = \frac{1}{2(\sigma^2+\pi_4^2)} + \frac{1}{4}[(1-r^2)(c_1+c_2+c_3) - (1+d_4)^2 c_4], \tag{54}$$

$$D_P = \frac{1}{2(\sigma^2+\pi_4^2)} - \frac{1}{4}[(1+r^2)(c_1+c_2+c_3) + (1+d_4)^2 c_4], \tag{55}$$

$$C = \frac{i\sigma\pi_4}{(\sigma^2+\pi_4^2)^2}, \tag{56}$$

with $s_k = \sin p_k$ and $c_k = \cos p_k$. By diagonalizing this matrix, we can derive an explicit form of physical meson propagators. We note that C gets zero in the chiral symmetric phase while it has nonzero values in the chiral broken phase.

We first check that pion mass becomes zero in the chiral-broken phase. For this purpose we substitute $p = (0, 0, 0, im_P)$ into the propagator. Then D_P is decoupled and the calculation gets simplified. We note that, in the chiral broken phase, the gap equation Eq. (8) gives $\sigma^2 + \pi_4^2 = 2/[3(1+r^2) + (1+d_4)^2]$. Pion mass in the chiral broken phase with $r = 1$ and $m = 0$ is derived from a pole of D_P with $p = (0, 0, 0, im_P)$ as

$$D_P(0,0,0,im_P) = \frac{3(1+r^2)+(1+d_4)^2}{4} - \frac{1}{4}((1+d_4)^2\cos(im_P) + 3(1+r^2)) = 0$$
$$\rightarrow \qquad \cosh(m_P) = 1. \tag{57}$$

This mode corresponds to a massless NG boson associated with SSB of chiral $U(1)$ symmetry, which is consistent with realistic QCD.

On the second-order phase boundary, a divergent correlation length in the critical behavior should produce another massless mode. We here show that the scalar meson becomes massless on the critical line. An inverse meson propagator matrix in general has off-diagonal components, but substitution of $p = (0, 0, 0, im_S)$ again decouples the scalar sector in the chiral-symmetric phase ($C = 0$). An explicit form of the scalar inverse propagator is given by Eq. (40). Then we derive the scalar mass from a pole of this propagator with $p = (0, 0, 0, im_S)$ as

$$D_S(0,0,0,im_S) = 0 \quad \rightarrow \quad \cosh m_S = 1 - \left[1 + \frac{3(1+r^2)}{(1+d_4)^2} + \frac{1}{(1+d_4)^2}\frac{2(\sigma^2-\pi_4^2)}{(\sigma^2+\pi_4^2)^2}\right]. \tag{58}$$

As seen from this, scalar meson has nonzero mass in general. On the phase boundary, however, we have $\sigma = 0$, $\pi_4 = -\bar{\mu}_3 + \sqrt{\bar{\mu}_3^2 + 2[3(1-r^2) - (1+d_4)^2]}$ and $\bar{\mu}_3 = \pm\frac{6r^2+2(1+d_4)^2}{\sqrt{6r^2+2(1+d_4)^2+6}}$ with $\bar{\mu}_3 = \mu_3 + 3r$. It leads to zero σ mass as

$$\cosh(m_S) = 1. \tag{59}$$

We can also show this from the chiral-broken phase. We have two massless modes only on the 2nd-order phase boundary, σ-meson and π-meson, which is inconsistent with the meson mass spectrum in QCD. We thus need to avoid this point in the simulation of QCD. In the first place this boundary corresponds to the boundary between the two-flavor and no-flavor ranges, which has the unphysical dispersion relation as shown in Sec. II. From the theoretical viewpoint, it is however an attractive topic. Further study including numerical simulations can elucidate detailed properties of this point.

Now let us discuss possibility of restoration of Lorentz symmetry. In the strong-coupling limit, what we can do is tuning of μ_3 and d_4 since we can ignore tuning for the plaquette action in this limit. However, we cannot restore the Lorentz symmetry correctly in this limit because of the large lattice artifacts. The A_4 meson propagator explicitly manifests this point as following: The A_4-sector propagator, which is diagonal even with finite spacial momentum, is given by Eq. (54). In the chiral-broken phase, we have $1/(\sigma^2 + \pi_4^2) = [3(1 + r^2) + (1 + d_4)^2]/2$. By substituting $p = (0, 0, 0, im_{A4})$, the pole of the propagator determines the axial vector meson mass as

$$\cosh m_{A_4} = 1 + \frac{6}{(1 + d_4)^2}. \tag{60}$$

For small but finite spatial momentum as $p = (p_1, p_2, p_3, iE)$, the pole of the propagator up to $O(p^2)$ gives

$$E^2 = m_{A_4}^2 + \frac{1 - r^2}{(1 + d_4)^2}\mathbf{p}^2. \tag{61}$$

It apparently indicates that we need to tune d_4 as $(1 + d_4)^2 = 1 - r^2$. However, for $r = 1$, the dependence on $\mathbf{p}$ itself disappears and the Lorentz symmetry cannot be restored. It is a typical strong-coupling artifact. Moreover, the tuned value of d_4 does not depend on μ_3, but it is also a lattice artifact. In the first place, the equation (8) indicates that π_4 always has a nonzero value in the physical parameter range ($\sigma \neq 0$) even if we tune μ_3 and d_4 independently except for $\mu_3 + 3r = 0$. All these results show that it is difficult to restore the symmetry in the physical parameter range within the framework of the strong-coupling QCD. We expect that it is just a strong-coupling artifact, and we can make π_4 zero and restore Lorentz symmetry in the weak coupling by tuning the three parameters appropriately.

In this section we have assumed the form of condensation $\sigma + i\gamma_4\pi_4$. As shown in the Appendix.A, we can also consider possibility of other condensations as $\sigma + i\gamma_4\pi_4 + i\gamma_5\pi_5$ or $\sigma + i\gamma_4\pi_4 + i\gamma_4\gamma_5\pi_{45}$. The results show that the solution with nonzero π_5 or π_{45} condensates cannot be a vacuum, and our solutions in this section are likely to be true vacua. We thus consider that the parity breaking phase will not appear in the KW fermion unless we introduce the flavored-mass terms shown in [32]. At the weak coupling there may be a more subtle competition between the discretization error and the counterterm. We thus need further study to conclude whether the parity breaking exist or not when we take into account all the three counterterms in the weak coupling.

In the end of this section, we discuss the other type of minimal-doubling fermions, called the Creutz-Borici type [15, 16]. We can analyze it in a parallel way. We note that this type specifies the diagonal direction characterized by $2\Gamma = \gamma_1 + \gamma_2 + \gamma_3 + \gamma_4$, instead of the time direction. Appendix. B is devoted to detailed analysis for this case. The result is qualitatively the same. We find two chiral boundaries and chiral condensate is nonzero between the boundaries.

IV. GROSS-NEVEU MODEL

We investigate the whole phase diagram for Karsten-Wilczek (KW) fermion by using the two-dimensional lattice Gross-Neveu model [40–49], which has common features with 4d lattice QCD. In two dimensions, massless KW fermion action is given by

$$aD_{\mathrm{KW}}(p) = i\sum_{\nu=1}^{2}\gamma_\nu \sin ap_\nu + i\gamma_2[r(1-\cos ap_1) + \mu + d\sin ap_2]. \tag{62}$$

In this section we concentrate on the case with $r = 1$. In this section we denote the relevant parameter μ_3 as just $\mu \equiv \mu_3$ and denote the maginal parameter d_4 as $d \equiv d_4$. To look into the number of flavors in a free theory, we for a while consider $d = 0$. For $-3 < \mu < -1$ and $-1 < \mu < 1$, there are only two zeros, and it becomes minimal-doubling. For $\mu < -3$ and $\mu > 1$, there is no zero, and it becomes a fermion-less theory. For $\mu = -3, 1$, there is one zero, but the dispersion relation becomes unphysical $\sim p_1 + p_2^2$. For $\mu = -1$, there two zeros but whose dispersion relation is again unphysical. The main difference from four-dimensional cases is that there is no 6-flavor range.

The lattice Gross-Neveu model with KW fermion is given by

$$\begin{aligned}S = {} & \frac{1}{2}\sum_{n,\nu}\bar{\psi}_n\gamma_\nu(\psi_{n+\nu} - \psi_{n-\nu}) + \frac{1}{2}\sum_n \bar{\psi}_n i\gamma_2(2\psi_n - \psi_{n+\hat{1}} - \psi_{n-\hat{1}}) \\ & - \frac{1}{2N}\sum_n [g_\sigma^2(\bar{\psi}_n\psi_n)^2 + g_2^2(\bar{\psi}_n i\gamma_2\psi_n)^2] \\ & + \mu\sum_n \bar{\psi}_n i\gamma_2\psi_n + d\sum_n \bar{\psi}_n i\gamma_2(\psi_{n+\hat{2}} - \psi_{n-\hat{2}}) + m\sum_n \bar{\psi}_n\psi_n,\end{aligned} \tag{63}$$

where ν stands for $\nu = 1, 2$, $n = (n_1, n_2)$ are the two dimensional coordinates and ψ_n stands for a N-component Dirac fermion field $(\psi_n)_j (j = 1, 2, ..., N)$. The bilinear $\bar{\psi}\psi$ means $\sum_{j=1}^{N}\bar{\psi}_j\psi_j$, and $(g_\sigma^2,\, g_2^2)$ corresponds to the 't Hooft couplings for the two types of four-fermi interactions. Here we define the two dimensional gamma matrices as $\gamma_1 = \sigma_1$, $\gamma_2 = \sigma_2$ and $\gamma_3 = \sigma_3$. We make all the quantities dimensionless in this equation. We consider scalar and time-direction vector four-fermi interactions, which are natural choices since KW fermion specifies the time direction. We note that, if we drop a mass term ($m = 0$), the action has $\pi/2$ discrete chiral symmetry, which can be spontaneously broken due to chiral condensate. By introducing auxiliary bosonic fields $\sigma(n)$, $\pi_2(n)$ we remove the four-point interactions as

$$\begin{aligned} S = & \frac{1}{2}\sum_{n,\nu}\bar{\psi}_n\gamma_\nu(\psi_{n+\nu}-\psi_{n-\nu}) - \sum_n \bar{\psi}_n i\gamma_2(\psi_{n+1}+\psi_{n-1}) + d\sum_n \bar{\psi}_n i\gamma_2(\psi_{n+\hat{2}}-\psi_{n-\hat{2}}) \\ & + \frac{N}{2}\sum_n [\frac{1}{g_\sigma^2}(\sigma(n)-m)^2 + \frac{1}{g_2^2}(\pi_2(n)-\mu-1)^2] + \sum_n \bar{\psi}_n[\sigma(n)+i\gamma_2\pi_2(n)]\psi_n. \end{aligned} \tag{64}$$

By solving the equations of motion, we show the following relation between these auxiliary fields and the bilinears of the fermion fields

$$\sigma(n) = m - \frac{g_\sigma^2}{N}\bar{\psi}\psi, \tag{65}$$

$$\pi_2(n) = 1 + \mu - \frac{g_2^2}{N}\bar{\psi}i\gamma_2\psi. \tag{66}$$

These relations indicate that σ and π_2 stand for the scalar and vector mesons. After integrating the fermion fields, the partition function and the effective action with these auxiliary fields are given by

$$Z = \int \prod_n d\sigma(n)d\pi_2(n)e^{-N S_{\rm eff}(\sigma,\pi_2)}, \tag{67}$$

$$S_{\rm eff}(\sigma,\pi_2) = \frac{1}{2}\sum_n[\frac{1}{g_\sigma^2}(\sigma(n)-m)^2 + \frac{1}{g_2^2}(\pi_2(n)-\mu-1)^2] - {\rm Tr}\,\log D_{n,m}, \tag{68}$$

with

$$\begin{aligned} D_{n,m} = & [\sigma(n)+i\gamma_2\pi_2(n)]\delta_{n.m} + \frac{\gamma_\mu}{2}(\delta_{n+\mu,m}-\delta_{n-\mu,m}) \\ & - \frac{i\gamma_2}{2}(\delta_{n+\hat{1},m}+\delta_{n-\hat{1},m}) + d\frac{\gamma_2}{2}(\delta_{n+\hat{2},m}-\delta_{n-\hat{2},m}). \end{aligned} \tag{69}$$

Here Tr stands for the trace both for the position and spinor spaces. As is well-known, the partition function in the Gross-Neveu model is given by the saddle point of this effective action in the large N limit. We denote as $\tilde{\sigma}(n)$, $\tilde{\pi}_2(n)$ solutions satisfying the saddle-point conditions

$$\frac{\delta S_{\rm eff}[\sigma(n),\pi_2(n)]}{\delta\sigma(n)} = \frac{\delta S_{\rm eff}[\sigma(n),\pi_2(n)]}{\delta\pi_2(n)} = 0. \tag{70}$$

Then the partition function is given by

$$Z = e^{-NS_{\rm eff}[\tilde{\sigma},\tilde{\pi_2}]}. \tag{71}$$

By assuming the translational invariance we define the position-independent solutions as $\sigma \equiv \tilde{\sigma}(0)$ and $\pi \equiv \tilde{\pi_2}(0)$ Then we can factorize a volume factor $V = \sum_n 1$ in the effective action as

$$\begin{aligned} S_{\text{eff}} &= V\tilde{S}_{\text{eff}}(\sigma, \pi_2), && (72) \\ \tilde{S}_{\text{eff}}(\sigma, \pi_2) &= \frac{1}{2g_\sigma^2}(\sigma - m)^2 + \frac{1}{2g_2^2}(\pi_2 - \mu - 1)^2 - \frac{1}{V}\text{Tr} \log D. && (73) \end{aligned}$$

We can write $\text{Tr}\log D$ in a simple form by the Fourier transformation to momentum space

$$\begin{aligned} \text{Tr} \log D &= V\int \frac{d^2k}{(2\pi)^2} \log[\det(\sigma + i\gamma_2\pi_2 + i\gamma_2((1+d)\sin k_2 - \cos k_1) + i\gamma_1 \sin k_1)] \\ &= V\int \frac{d^2k}{(2\pi)^2} \log[\sigma^2 + (\pi_2 + (1+d)\sin k_2 - \cos k_1)^2 + (\sin k_1)^2], && (74) \end{aligned}$$

with det being the determinant in the spinor space. Now saddle-point equations are written as

$$\begin{aligned} \frac{\delta\tilde{S}_{\text{eff}}}{\delta\sigma} &= \frac{(\sigma - m)}{g_\sigma^2} - 2\int \frac{d^2k}{(2\pi)^2} \frac{\sigma}{\sigma^2 + (\pi_2 + (1+d)\sin k_2 - \cos k_1)^2 + (\sin k_1)^2} = 0, && (75) \\ \frac{\delta\tilde{S}_{\text{eff}}}{\delta\pi_2} &= \frac{\pi_2 - \mu - 1}{g_2^2} - 2\int \frac{d^2k}{(2\pi)^2} \frac{\pi_2 + (1+d)\sin k_2 - \cos k_1}{\sigma^2 + (\pi_2 + (1+d)\sin k_2 - \cos k_1)^2 + (\sin k_1)^2} = 0. && (76) \end{aligned}$$

Here the values of σ and π_2 in the vacuum are determined as $\sigma(\mu, d, g_\sigma^2, g_2^2, m)$, $\pi_2(\mu, d, g_\sigma^2, g_2^2, m)$ from the saddle-point equations once μ, d, g_σ^2, g_2^2 and m are fixed.

Let us look into the phase diagram with respect to chiral symmetry. We here consider a massless case as $m = 0$ to have the exact discrete chiral symmetry in the action. To capture rough structure of the phase diagram, we first take the simplest case with $d = 0$ and $g_\sigma^2 = g_2^2 \equiv g^2$. Nonzero d just gives slight change of the phase diagram. Since a single coupling constant works when we study the Aoki phase in the Wilson fermion [27], we expect that the above condition for the couplings works at least for deriving rough phase structure. The order parameter is σ, which can be zero or non-zero depending on values of μ and g^2. The phase boundary is determined by imposing $\sigma = 0$ on Eq. (75)(76) after the overall σ being removed in Eq. (75). Then the conditions for the phase boundary are given by gap equations as

$$\begin{aligned} \frac{\pi_2 - \mu_c - 1}{g^2} &= 2\int \frac{d^2k}{(2\pi)^2} \frac{\pi_2 + \sin k_2 - \cos k_1}{(\pi_2 + \sin k_2 - \cos k_1)^2 + (\sin k_1)^2}, && (77) \\ \frac{1}{g^2} &= 2\int \frac{d^2k}{(2\pi)^2} \frac{1}{(\pi_2 + \sin k_2 - \cos k_1)^2 + (\sin k_1)^2}, && (78) \end{aligned}$$

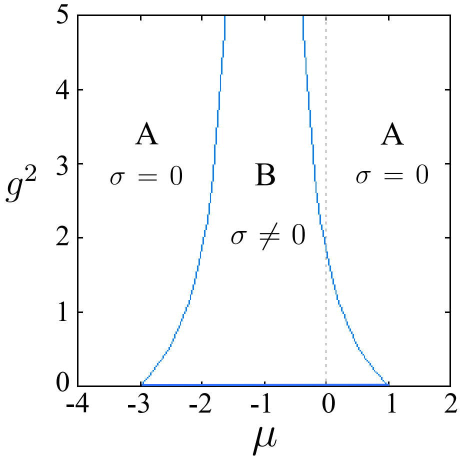

FIG. 6: Chiral phase diagram for KW Gross-Neveu model in the μ-g^2 space. A stands for the chiral symmetric phase. B stands for the chiral-broken phase. The chiral boundaries are connected to the edges of minimal-doubling ranges.

with μ_c being a critical value of μ. Here we derive the chiral phase boundary $\mu_c(g^2)$ as a function of the coupling g^2 by getting rid of vector condensate π_2 from these equations. The phase diagram is depicted in Fig. 6. A stands for the chiral symmetric phase $\sigma = 0$ and B for chiral broken phase $\sigma \neq 0$. For $-2 < \pi_2 < 2$ the integral in Eq.(78) diverges, which leads to the critical lines with zero gauge coupling for $-3 < \mu < 1$ as shown in Fig. 6. This is reasonable since the weak-coupling limit should have zero chiral condensate. As we expected, the chiral critical line is connected to boundaries between two-flavor and no-flavor phases in the weak-coupling limit ($\mu = -3, 1$). It is consistent with our intuition that the fermion-less theory cannot cause spontaneous breaking of chiral symmetry. We can check the mass of the scalar meson mass becomes zero on the critical line $\mu_c(g^2)$. The mass of σ is calculated analytically on the boundary, and is shown to be zero as

$$\begin{aligned} m_\sigma^2 &\propto \langle \frac{\delta^2 S_{\text{eff}}}{\delta\sigma(n)\delta\sigma(m)} \rangle_{\mu_c} = V \frac{\delta^2 \tilde{S}_{\text{eff}}}{\delta^2\sigma^2}|_{\mu_c} \\ &= V\Big[\frac{1}{g^2} - 2\int \frac{d^2k}{(2\pi)^2} \frac{1}{\sigma^2 + (\pi_2 + \sin k_2 - \cos k_1)^2 + (\sin k_1)^2} \\ &\qquad\qquad - 4\sigma^2 \int \frac{d^2k}{(2\pi)^2} \frac{1}{\sigma^2 + (\pi_2 + \sin k_2 - \cos k_1)^2 + (\sin k_1)^2}\Big]_{\mu_c} \\ &= 0. \end{aligned} \tag{79}$$

A massless scalar meson indicates that the phase boundary we derived is a second-order critical line. This result is consistent with the strong-coupling lattice QCD in the previous section.

Next, we discuss more general cases with $d \neq 0$ and $g_\sigma^2 \neq g_2^2$. Nonzero values of d change $\sin k_2 \to (1+d)\sin k_2$ in (77)(78) and give just qualitative changes of the phase diagram: Since the minimal-doubling ranges are given by $-1 < \mu < 1+d$ and $-3-d < \mu < -1$ for nonzero d, it gives a larger physical range in the phase diagram. As an example, we depict the μ-g^2 phase diagram for $d = 0.5$ in Fig. 7. In the case with two independent coupling constants $g_\sigma^2 \neq g_2^2$, the equations for the phase boundary are given by

$$\mu_c + 1 \;=\; \pi_2 \left(1 - \frac{g_2^2}{g_\sigma^2}\right) - 2g_2^2 \int \frac{d^2k}{(2\pi)^2} \frac{\pi_2 + \sin k_2 - \cos k_1}{(\pi_2 + \sin k_2 - \cos k_1)^2 + (\sin k_1)^2}, \tag{80}$$

$$\frac{1}{g_\sigma^2} \;=\; 2\int \frac{d^2k}{(2\pi)^2} \frac{1}{(\pi_2 + \sin k_2 - \cos k_1)^2 + (\sin k_1)^2}. \tag{81}$$

In this case the phase diagram is deformed to some extent: If we fix one of the coupling constants and depict the phase diagram, the physical phase gets larger toward the strong-coupling limit while it gets narrower at the weak-coupling. As an example, we depict the μ-g_σ^2 phase diagram for $g_2^2 = 1.0$ in Fig. 8. Since we have already shown that the physical phase gets rather narrower in the strong-coupling limit in 4d lattice QCD in Sec. III. it is natural to consider that the single-coupling GN model in Fig. 6 is sufficient to mimic 4d QCD at least for investigating the chiral phase diagram. We note that we can introduce two more types of four-point interactions in the GN action (63) as $(\bar{\psi}_n i\gamma_1 \psi_n)^2$ and $(\bar{\psi}_n i\gamma_3 \psi_n)^2$, which give π_1 and π meson fields. Both vacuum expectation values of π_1 and π, if they are nonzero, cause spontaneous parity symmetry breaking. However, by comparing the effective potentials or solving four gap equations ($\frac{\delta \tilde{S}_{\rm eff}}{\delta\sigma} = 0$, $\frac{\delta \tilde{S}_{\rm eff}}{\delta\pi_1} = 0$, $\frac{\delta \tilde{S}_{\rm eff}}{\delta\pi_2} = 0$, $\frac{\delta \tilde{S}_{\rm eff}}{\delta\pi} = 0$), we can clearly show that they have zero vacuum expectation values as in the case of the strong-coupling lattice QCD in Appendix.A. Instead of solving all the gap equations numerically, we here show the consistency check on $\pi_1 = 0$. From two saddle-point equations $\frac{\delta \tilde{S}_{\rm eff}}{\delta\sigma} = 0$ and $\frac{\delta \tilde{S}_{\rm eff}}{\delta\pi_1} = 0$ we derive one equation,

$$0 = 2\int \frac{d^2k}{(2\pi)^2} \frac{\sin k_1}{\sigma^2 + \pi^2 + (\pi_2 + (1+d)\sin k_2 - \cos k_1)^2 + (\pi_1 + \sin k_1)^2}. \tag{82}$$

If we take $\pi_1 = 0$, the right-hand side becomes an odd function of k_1, and the above equation holds identically. We can also show from the gap equations that $\pi = 0$ is preferred. These

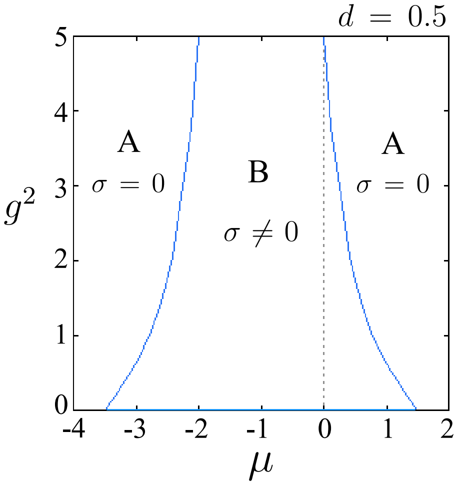

FIG. 7: Chiral phase diagram for KW Gross-Neveu model in the μ-g^2 space with $d = 0.5$ ($g^2 \equiv g_\sigma^2 = g_2^2$). The physical (minimal-doubling) phase with chiral condensate is enlarged by nonzero values of d.In the weak-coupling limit, the minimal-doubling phases are given by $-3.5 < \mu < -1$ and $-1 < \mu < 1.5$.

results mean that the parity-broken vacuum is not preferred, and as long as we consider the vacuum of the theory, the two four-fermi interactions in (63) are sufficient. We next show that, however, we have to take into account the excitation of π_1 and π to investigate the Lorentz symmetry restoration in the GN model.

By now we have considered only the vacuum of the theory. Although it works to elucidate the chiral phase structure, we need look into excitations from the vacuum in order to investigate renormalization for the rotation symmetry restoration. By expanding the mesonic action up to the 2nd order, we can derive the meson propagator matrix for $\sigma, \pi_1, \pi_2, \pi$ as in the strong-coupling lattice QCD in Sec. III. By diagonalizing this 4×4 matrix, we obtain the proper propagators. Then, we can discuss how the rotation symmetry can be restored by tuning the parameters including μ, d, g_σ^2 and g_2^2. Although we can perform this procedure in principle, all the matrix components include complicated momentum integrals in this case. Moreover, we need to substitute the VEV of meson fields derived from the gap equations, which also require numerical integrals. We consider that these numerical calculations are beyond the scope of this study, but the future work should be devoted to it. Instead, we here show a process of deriving the dispersion relations in details in the following. The meson

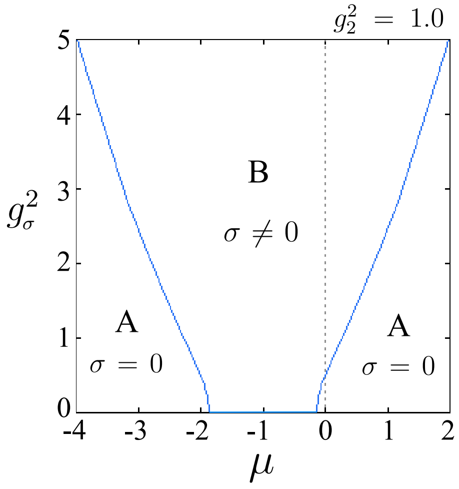

FIG. 8: Chiral phase diagram for KW Gross-Neveu model in the μ-g_σ^2 space with $g_2^2 = 1.0$ ($d = 0$). The physical (minimal-doubling) phase with chiral condensate gets larger toward the strong-coupling limit.

excitations from the vacuum are given by

$$\sigma = \bar{\sigma} + \sigma(n), \quad \pi_1 = \bar{\pi}_1 + \pi_1(n), \quad \pi_2 = \bar{\pi}_2 + \pi_2(n), \quad \pi = \bar{\pi} + \pi(n), \tag{83}$$

where VEVs ($\bar{\sigma}$, $\bar{\pi}_1$, $\bar{\pi}_2$, $\bar{\pi}$) are determined by the gap equations. We have already shown $\bar{\pi}_1 = \bar{\pi} = 0$ while $\bar{\sigma}$ and $\bar{\pi}_2$ depends on the parameters. The Dirac operator with these excitations are written as

$$D_{n,m} = (\mathcal{S}_0^{-1})_{n,m} + \mathcal{M}(n)\delta_{n,m}, \tag{84}$$

$$\begin{aligned}(\mathcal{S}_0^{-1})_{n,m} = [\bar{\sigma} + i\gamma_2\bar{\pi}_2]\delta_{n.m} + \frac{\gamma_\mu}{2}(\delta_{n+\mu,m} - \delta_{n-\mu,m})/a \\ - \frac{i\gamma_2}{2}(\delta_{n+\hat{1},m} + \delta_{n-\hat{1},m})/a + d\frac{\gamma_2}{2}(\delta_{n+\hat{2},m} - \delta_{n-\hat{2},m})/a\end{aligned} \tag{85}$$

$$\mathcal{M}(n) = \sigma(n) + i\gamma_1\pi_1(n) + i\gamma_2\pi_2(n) + i\gamma_3\pi(n), \tag{86}$$

where we make the lattice spacing a manifest. Note $\sigma, \pi_1, \pi_2, \pi \sim O(1/a)$. For completeness, we consider the following action including four independent coupling constants,

$$S_{\text{eff}} = \sum_n [\frac{1}{2g_\sigma^2}(\sigma - m)^2 + \frac{1}{2g_1^2}\pi_1^2 + \frac{1}{2g_2^2}(\pi_2 - \mu - 1)^2 + \frac{1}{2g_\pi^2}\pi^2] - \text{Tr}\,\log[\mathcal{S}_0^{-1}(1 + \mathcal{S}_0\mathcal{M})]_{n,m}. \tag{87}$$

Tr is a trace for coordinate and spinor spaces. By expanding this expression up to second order of mesonic fluctuations, we derive the effective action up to the quadratic order as

$$S_{\text{eff}} = S_{\text{eff}}^{(0)} + S_{\text{eff}}^{(2)} + \cdots, \tag{88}$$

with

$$S_{\text{eff}}^{(2)} = \sum_n \left[\frac{\sigma(n)^2}{2g_\sigma^2} + \frac{\pi_1(n)^2}{2g_1^2} + \frac{\pi_2(n)^2}{2g_2^2} + \frac{\pi^2(n)}{2g_\pi^2} + \frac{1}{2}\mathrm{tr}\sum_m \mathcal{S}_0(m,n)\mathcal{M}(n)\mathcal{S}_0(n,m)\mathcal{M}(m) \right], \tag{89}$$

with tr is a trace for the spinor space. By fourier transformation we can derive the form in the momentum space as

$$\begin{aligned} S_{\text{eff}}^{(2)} = \int_{-\pi/a}^{\pi/a} \frac{d^2p}{(2\pi)^2} \Big[\frac{\sigma(p)^2}{2g_\sigma^2} + \frac{\pi_1(p)^2}{2g_1^2} + \frac{\pi_2(p)^2}{2g_2^2} + \frac{\pi(p)^2}{2g_\pi^2} \\ + \frac{1}{2}\mathrm{tr}\int_{\pi/a}^{\pi/a} \frac{d^2k}{(2\pi)^2} \mathcal{S}_0(p+k)\mathcal{M}(p)\mathcal{S}_0(k)\mathcal{M}(-p) \Big], \end{aligned} \tag{90}$$

with

$$\mathcal{S}_0(k) = \frac{1}{\det(\mathcal{S}_0^{-1}(k))} \left[\bar{\sigma} - i\gamma_2 \left(\bar{\pi}_2 + (1+d)\frac{\sin ak_2}{a} + \frac{\cos ak_1}{a} \right) - i\gamma_1 \frac{\sin ak_1}{a} \right], \tag{91}$$

$$\det(\mathcal{S}_0^{-1}(k)) = \bar{\sigma}^2 + \left(\bar{\pi}_2 + (1+d)\frac{\sin ak_2}{a} - \frac{\cos ak_1}{a} \right)^2 + \left(\frac{\sin ak_1}{a} \right)^2. \tag{92}$$

Finally, the mesonic propagator matrix is given by

$$\mathcal{D}_{XY}(p) = \frac{\delta^2 S_{\text{eff}}^{(2)}}{\delta\mathcal{M}_X(p)\delta\mathcal{M}_Y(-p)} \tag{93}$$

where X and Y stand for one of channels σ, π_1, π_2 and π. For example, $\mathcal{D}_{\sigma\sigma}(p)$ is given by

$$\begin{aligned} \mathcal{D}_{\sigma\sigma}(p) = & \frac{1}{g_\sigma^2} + \int_{\pi/a}^{\pi/a} \frac{d^2k}{(2\pi)^2} \frac{1}{\det[\mathcal{S}_0^{-1}(p+k)\mathcal{S}_0^{-1}(k)]} \times \Big[\bar{\sigma}^2 \\ & - \Big(\bar{\pi}_2 + (1+d)\frac{\sin ak_2}{a} + \frac{\cos ak_1}{a} \Big) \Big(\bar{\pi}_2 + (1+d)\frac{\sin a(p_2+k_2)}{a} + \frac{\cos a(p_1+k_1)}{a} \Big) \\ & - \frac{\sin ak_1 \sin a(p_1+k_1)}{a^2} \Big]. \end{aligned} \tag{94}$$

In the same way we can derive all other 16 components of the matrix, all of which take nonzero values in general. What we are interested in is terms of the components up to $O(p^2)$ as far as we consider the rotation symmetry up to $O(a)$ discretization errors. The coefficients can be extracted through numerical integrals of the equations as (94). We note that we also need to substitute into the integral the values of VEV of σ and π_2 derived from the gap equations. Then we diagonalize the 4×4 meson matrix $\mathcal{D}_{XY}$ to derive the proper meson propagator. By introducing $p = (\mathbf{p}, iE)$ into the propagators, we find the dispersion relations. The question is which parameters among μ, d, g_σ^2, g_1^2, g_2^2, g_π^2 need to be tuned to recover Lorentz symmetry. It can give an important suggestion to lattice QCD with the minimal-doubling fermions. We devote a future work to this analysis.

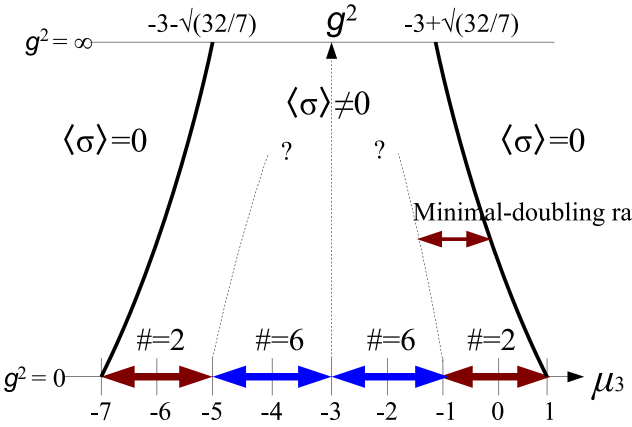

FIG. 9: Conjecture on μ_3-g^2 chiral phase structure for Karsten-Wilczek fermion with r=1. The width of the minimal-doubling range determines how hard it is to tune μ_3.

V. CONJECTURE ON PHASE STRUCTURE IN QCD

From the study of strong-coupling lattice QCD and the Gross-Neveu model we speculate on the whole chiral phase structure in lattice QCD with Karsten-Wilczek fermion. Fig. 9 is a conjectured chiral phase structure with the number of flavors in the μ_3-g^2 space for $r = 1$. There are roughly two phases with and without chiral condensate, or equivalently with and without SSB of chiral symmetry. As was shown in the previous section, the boundary between chiral symmetric and broken phases starts from the edge of the two-flavor region of the free theory. We expect that the chiral boundaries are connected to the two-flavor and no-flavor phases also in 4d QCD as shown in Fig. 9.

The question is a boundary between two-flavor and six-flavor ranges. In the weak-coupling limit ($g^2 = 0$) we analytically know the number of physical flavors: There are four sectors with two, six, six and two flavors. There are only no flavors of fermions outside these ranges. Toward the strong coupling, these ranges will change with g^2 as shown in Fig. 9. We have seen that we cannot distinguish two-flavor and six flavor ranges in the strong-coupling limit, which means that the number of species becomes an ambiguous notion in this limit. We thus expect that the boundary disappears at a certain gauge coupling, and the two-flavor and six-flavor regions become undistinguishable as shown in Fig. 9.

From the viewpoints of practical application to two-flavor QCD, the relevant parameter

μ_3 has to be tuned to cancel the $O(1/a)$ imaginary chemical potential renormalization for the two flavors. One necessary condition (but not a sufficient condition) for this purpose is to set μ_3 in the minimal-doubling range to realize the two-flavor QCD. As we conjectured in Fig. 9, the minimal-doubling range in the middle gauge coupling should have some width. One possible indicator of the minimal-doubling phase is the pion spectrum: If μ_3 is in the no-flavor range, there is no SSB of chiral symmetry and no massless pion. If μ_3 gets into the six-flavor region, the number of pseudo Nambu-Goldstone bosons increases. However, setting μ_3 in the minimal-doubling range is not sufficient for physical QCD to be described: The Lorentz symmetric dispersion relation is broken down for general values of μ_3 in the minimal-coupling range as shown in Eq. (11) and below for a free theory.

$$D(p) \sim i\gamma_i p_i + i\gamma_4 p_4 \sqrt{(1+d_4)^2 - \mu_3^2} + O(ap^2). \tag{95}$$

Since this free-theory argument indicates that the rotation symmetry can be restored by tuning d_4 as $(1+d_4)^2 - \mu_3^2 = 1$, we may be able to restore Lorentz symmetry just by tuning d_4 with μ_3 being set in the minimal-doubling range. Note that the minimal-doubling range gets larger with nonzero d_4 as shown in Sec.III and IV, thus it seems that proper tuning of d_4 can be done for any value of μ_3 without breaking down minimal-doubling. (We need one more parameter tuning for the plaquette action in any case.) We also emphasize that the same relative tuning of μ_3 and d_4 makes tree level couplings of the gauge field to the fermions have a correct Lorentz-symmetric form. To show this, we look into the quark-quark-gluon vertex at the tree level. For the case of $\mu_3 = 0$ and $d_4 = 0$ it is given by

$$V(p,k) = -ig_0 \left(\gamma_\mu \cos\frac{a(p_\mu + k_\mu)}{2} + \gamma_4 (1-\delta_{\mu 4}) \sin\frac{a(p_\mu + k_\mu)}{2} \right), \tag{96}$$

as shown in [26]. For nonzero μ_3 and d_4, it is modified as

$$V(p,k) = -ig_0 \left(\sum_{j=1}^{3} \gamma_j \cos\frac{a(p_j + k_j)}{2} + \gamma_4 \left[(1+d_4)\cos\frac{a(p_4 + k_4)}{2} + \sum_{i=1}^{3} \sin\frac{a(p_i + k_i)}{2} \right] \right), \tag{97}$$

where we have no direct emergence of μ_3 since it is a parameter for onsite (non-hopping) terms. However, as we discussed, the zeros of the Dirac operator for nonzero μ_3 and d_4 is given by a function of μ_3 and d_4 as $\bar{p} = \bar{k} = (0,0,0,\frac{1}{a}\arcsin(-\frac{\mu_3}{1+d_4}))$. Now we expand both p and k about the zeros as $p \to \bar{p} + p$ and $k \to \bar{k} + k$. In particular, the coefficient of γ_4 in

(97) is expanded as

$$\begin{aligned}
&(1+d_4)\Big[\cos\frac{a(\bar{p}_4+\bar{k}_4)}{2}\cos\frac{a(p_4+k_4)}{2}-\sin\frac{a(\bar{p}_4+\bar{k}_4)}{2}\sin\frac{a(p_4+k_4)}{2}\Big]+\sum_{i=1}^{3}\sin\frac{a(p_i+k_i)}{2}\\
=&(1+d_4)\Big[\sqrt{1-\frac{\mu_3}{(1+d_4)^2}}\cos\frac{a(p_4+k_4)}{2}+\frac{\mu_3}{1+d_4}\sin\frac{a(p_4+k_4)}{2}\Big]+\sum_{i=1}^{3}\sin\frac{a(p_i+k_i)}{2}\\
=&(1+d_4)\sqrt{1-\frac{\mu_3}{(1+d_4)^2}}+O(ap,ak), \qquad (98)
\end{aligned}$$

Then, the vertex surviving in the naive continuum limit is given by

$$V(p,k)=-ig_0\left(\gamma_1+\gamma_2+\gamma_3+\gamma_4\sqrt{(1+d_4)^2-\mu_3^2}\right)+O(ap,ak). \qquad (99)$$

Here we omit the ± sign in front of γ_4 for the doubler pairs for simplicity. It is now obvious that the tuning condition for the speed of light $(1+d_4)^2-\mu_3^2=1$ also fixes the couplings of the gauge fields to the fermion fields in the tree level up to the discretization errors. At least in the naive continuum limit, we can have a correct set of the Feynman rules for fermion fields with the condition. However it is too early to conclude that this condition is sufficient for Lorentz symmetry restoration since all the other Ward identities may not be corrected by it in the interacting theory including the loop effects: To discuss details, we consider the quark self-energy in lattice QCD with minimal-doubling fermions following [26] as

$$\Sigma(p,m)=i\gamma_\mu p_\mu\Sigma_1(p)+m\Sigma_2(p)+d_1(g_0)\cdot i\gamma_4 p_4+d_2(g_0)\cdot i\frac{\gamma_4}{a}, \qquad (100)$$

where Σ_1, Σ_2, d_1 and d_2 can be calculated in the perturbative analysis. It is clear that μ_3 and d_4 corresponds to counter parameters for d_2 and d_1 respectively, and the Dirac operator (95) is renormalized as $d_4\to d_4+d_1$ and $\mu_3\to\mu_3+d_2$ in the interacting theory. The last term with d_2, or the $O(1/a)$ renormalization, causes a shift of the poles of the Dirac propagator away from their original positions as well as the change of the speed of light as shown in (95). In the present work, we have also shown that this contribution changes the size of the minimal-doubling range at the finite gauge coupling and provides the non-trivial phase structure as shown in Fig. 9. The question is whether or not we need to move the poles of the propagator back to the tree-level positions by tuning μ_3 for a correct continuum limit. As far as the dispersion relation can be restored by d_4, it seems that the position of poles is not relevant to physics. However, in practical use of the minimal-doubling fermion, d_4 should be also tuned to make the conserved charge unity as shown in [26]. It is not obvious whether this condition can also fix the speed of light non-perturbatively. More generally speaking, it is very nontrivial whether all the Ward identities are fixed only by one tuning condition in the interacting theory. If we cannot restore Lorentz symmetry only with d_4 tuning unlike the free theory, it means that we still need to fine-tune the three parameters independently for a correct continuum limit of lattice QCD simulations [24–26]. Further study is needed to figure out this point.

In the end of this section, we comment on another possibility for studying minimal-doubling fermions. One interesting possibility is the chiral perturbation theory for minimal-doubling fermions. Although we expect that it is quite tedious to construct the minimal-doubling ChPT with the lower discrete symmetry than Wilson and staggered fermions, the process could have some similarities with that of the in-medium ChPT [50]. If we succeed to construct the minimal-doubling ChPT, it is intriguing to consider the Lorentz symmetry restoration within the theory and discuss the parameter tuning for the symmetry restoration. We can also investigate the vacuum and the phase structure in the theory. We devote future works to the study on the minimal-doubling ChPT.

VI. SUMMARY AND DISCUSSION

In this paper we investigate the chiral phase structure in the parameter space for lattice QCD with minimal-doubling fermions, which can be seen as lattice fermions with a species-dependent naive chemical potential term. We study the phase structure with Karsten-Wilczek fermion by using strong-coupling lattice QCD and the Gross-Neveu model, and find out the nontrivial chiral phase structure in the $\mu_3 - g^2$ plane.

In Sec. II, we have proposed flavored-chemical-potential lattice fermions, where some of doublers are eliminated by a species-dependent chemical potential term without losing all chiral symmetries. Minimal-doubling fermions are shown to be a special case of this type. In Sec. III we investigate the chiral phase structure of lattice QCD with Karsten-Wilczek fermions in the strong-coupling regime. We derive an effective action for the scalar and 4th vector fields, and find that chiral symmetry is spontaneously broken in a certain range of the relevant parameter μ_3 while the chiral condensate becomes zero outside the range. We show that there is a 2nd-order phase transition between chiral symmetric and broken phases as a function of μ_3. We also show that pion becomes massless as a Nambu-Goldstone boson in the chiral-broken phase while the scalar meson becomes massless only on the second-order phase boundary due to the critical behavior. In Sec. IV we obtain information on the whole chiral phase structure in the $\mu_3 - g^2$ space by using the Gross-Neveu model with KW fermion in large N limit. From the gap equations we derive a chiral phase diagram. In Sec V we discuss the whole phase structure in 4-dimensional lattice QCD with KW fermions. We conjecture the chiral phase structure and numbers of massless flavors in the phase diagram. We also discuss the fine-tuning process of μ_3 in lattice QCD from the viewpoint of the minimal-doubling range of the conjectured phase diagram.

In this paper we have investigated whether or not chiral symmetry is spontaneously broken depending on the parameters. Unlike Wilson parity-flavor breaking phase with the width $m \sim O(a^3)$ [29], it seems that we do not have fine phase structures in the weak-coupling regime as shown in Fig. 9. It is because the chiral symmetry breaking is physical, and there is no competition between the relevant parameter and the lattice artifact, which did cause the Aoki phase or the Creutz-Sharpe-Singleton phase in Wilson fermion [29, 30]. Although our analysis on chiral symmetry and that on parity symmetry in Wilson have some common features, they are on the different levels.

In this work, we do not take much care of π_4 condensate nor its physical implication. As we discussed in Sec. III this condensate is likely to be related to the (pseudo) quark density. On the other hand, Eq. (8) in the strong-coupling limit shows that π_4 is nonzero for any values of μ_3 and d_4 except for the unphysical point $\mu_3 + 3r = 0$. We consider that it is just a strong-coupling artifact, and the π_4 condensate can be eliminated by fine-tuning all the three parameters appropriately in the weak coupling. There is possibility that another way of introducing the dimension-4 counterterm as an O(1) imaginary chemical potential term $\bar{\psi}_n \gamma_4 (e^{i\mu}\psi_{n+4} - e^{-i\mu}\psi_{n-4})$ may work since the flavored-chemical-potential term could generate $O(1)$ effective imaginary chemical potential too.

In the end of this paper, we refer to a future work. We can apply the flavored-chemical-potential (FCP) fermions to finite-temperature and finite-density lattice QCD, and obtain finite-(T,μ) QCD phase diagram. In our next work [51], we will propose a new method to study lattice QCD in medium by using FCP fermion formulations.

Acknowledgments

TM is thankful to M. Creutz, T. Kimura and A. Ohnishi for fruitful discussion and hearty encouragement. The author also thanks F. Karsch for the discussion. The author appreciates the technical help by T. Kawanai. TM is supported by Grant-in-Aid for Japan Society for the Promotion of Science (JSPS) Postdoctoral Fellows for Research Abroad(No.24-8).

Appendix A: Possibility of pion condensation

We here assume a form of meson condensate with chiral, 4th vector and pion condensates as

$$\mathcal{M}_0 = \sigma \mathbf{1}_4 + i\pi_4\gamma_4 + i\pi_5\gamma_5. \tag{A1}$$

The effective potential for σ, π_4 and π_5 is given by

$$\begin{aligned}\mathcal{V}_{\text{eff}}(\sigma,\pi_4,\pi_5) = {} & \frac{1}{2}\log(\sigma^2+\pi_4^2+\pi_5^2) - m\sigma + (\mu_3+3r)\pi_4 \\ & -\frac{1}{4}[3(1+r^2)+(1+d_4)^2]\sigma^2 - \frac{1}{4}[3(1-r^2)-(1+d_4)^2]\pi_4^2 - \frac{1}{4}[3(1+r^2)+(1+d_4)^2]\pi_5^2.\end{aligned} \tag{A2}$$

We now find saddle points of $\mathcal{V}_{\text{eff}}$ given by

$$\frac{3(1+r^2)+(1+d_4)^2}{2}\sigma + m - \frac{\sigma}{\sigma^2+\pi_4^2+\pi_5^2} = 0\,, \tag{A3}$$

$$\frac{3(1-r^2)-(1+d_4)^2}{2}\pi_4 - (\mu_3+3r) - \frac{\pi_4}{\sigma^2+\pi_4^2+\pi_5^2} = 0\,, \tag{A4}$$

$$\frac{3(1+r^2)+(1+d_4)^2}{2}\pi_5 - \frac{\pi_5}{\sigma^2+\pi_4^2+\pi_5^2} = 0. \tag{A5}$$

We now consider a case for $r=1$, $d_4=0$ and $m=0$. We have two types of solutions as $\pi_5=0$ and $\pi_5\neq 0$. For $\pi_5=0$, we have the two solutions $\mathcal{M}_0^A$ and $\mathcal{M}_0^B$ in (29)(30) as we discussed in Sec. III. For $\pi_5\neq 0$, (A4)(A5) give $\sigma^2+\pi_4^2+\pi_5^2 = 2/7$ and $\pi_4 = -\bar{\mu}_3/4 = -(\mu_3+3)/4$. By substituting them into (A2) the effective potential as a function of $\bar{\mu}_3$ is given by

$$\mathcal{V}_{\text{eff}}(\pi_5\neq 0) = \frac{1}{2}\log\frac{2}{7} - \frac{1}{2} - \frac{1}{8}\bar{\mu}_3^2. \tag{A6}$$

On the other hand, for example, the effective potential for one of $\pi_5=0$ solutions $\mathcal{M}_0^B$ is given by

$$\mathcal{V}_{\text{eff}}(\pi_5=0,\mathcal{M}_0^B) = \frac{1}{2}\log\frac{2}{7} - \frac{1}{2} - \frac{1}{8}\bar{\mu}_3^2. \tag{A7}$$

It is obvious $\mathcal{V}_{\rm eff}(\pi_5 \neq 0) \not< \mathcal{V}_{\rm eff}(\pi_5 = 0, \mathcal{M}_0^B)$ for any value of $\bar{\mu}_3$. It indicates that the $\pi_5 \neq 0$ solution is unlikely to be a vacuum. We thus conclude that, at least in this framework, there is no pion condensate or no spontaneous parity symmetry breaking. We also perform the same analysis for the condensate form $\sigma \mathbf{1}_4 + i\pi_4\gamma_4 + i\pi_{45}\gamma_{45}$, and will find that $\pi_{45} \neq 0$ is not a vacuum of the theory.

Appendix B: Creutz-Borici case

A free action of Creutz-Borici fermion is given by

$$\begin{aligned} S_{\rm BC} = \sum_n [\frac{1}{2}\sum_\mu \bar{\psi}_n(\psi_{n+\mu} - \psi_{n-\mu}) + \frac{ir}{2}\sum_\mu \bar{\psi}_n(\Gamma - \gamma_\mu)\,(2\psi_n - \psi_{n+\hat{\mu}} - \psi_{n-\hat{\mu}}) \\ + ic_3\bar{\psi}_n\Gamma\psi_n + m\bar{\psi}_n\psi_n]\,, \end{aligned} \tag{B1}$$

$$\Gamma = \frac{1}{2}\sum_\mu \gamma_\mu, \quad \gamma'_\mu = \Gamma\gamma_\mu\Gamma = \Gamma - \gamma_\mu, \tag{B2}$$

where c_3 corresponds to μ_3 in Karsten-Wilczek fermion and Γ satisfies $\Gamma^2 = 1$ and $\{\Gamma, \gamma_\mu\} = 1$. In this case we have onsite operator and projection operators as $\hat{M} = m\mathbf{1}_4 + i(c_3 - 2r)\Gamma^{\rm T}$ and

$$P_\mu^+ \;=\; \frac{1}{2}\{\gamma_\mu(1+ir) + ir\Gamma\}, \quad P_\mu^- = \frac{1}{2}\{\gamma_\mu(1-ir) - ir\Gamma\}. \tag{B3}$$

The strong-coupling analysis is done in a parallel manner to KW fermion. By taking $\mathcal{M} = \sigma + i\pi_\Gamma\Gamma$, the corresponding gap equations become

$$2(1+r^2)\sigma + m - \frac{\sigma}{\sigma^2 + \pi_\Gamma^2} \;=\; 0\,, \tag{B4}$$

$$(1+r^2)\pi_\Gamma - (c_3 + 2r) - \frac{\pi_\Gamma}{\sigma^2 + \pi_\Gamma^2} \;=\; 0\,, \tag{B5}$$

For $m = 0$, equations for second-order phase boundaries are given by

$$2(1+r^2) - \frac{1}{\pi_\Gamma^2} \;=\; 0\,, \tag{B6}$$

$$(1+r^2)\pi_\Gamma - (c_3 + 2r) - \frac{1}{\pi_\Gamma} \;=\; 0\,, \tag{B7}$$

Then chiral boundaries are given by

$$c_3 = \pm\frac{\sqrt{1+r^2}}{\sqrt{2}} - 2r. \tag{B8}$$

For $r = 1$ chiral condensate is nonzero and chiral symmetry is spontaneously broken for $-3 < c_3 < -1$.

---

[1] L. H. Karsten and J. Smit, Nucl. Phys. B **183**, 103 (1981).

[2] H. B. Nielsen and M. Ninomiya, Nucl. Phys. B **185**, 20 (1981); Nucl. Phys. B **193** 173 (1981); Phys. Lett. B **105** 219 (1981).

[3] K. G. Wilson, Phys. Rev. D **10**, 2445 (1974).

[4] D. B. Kaplan, Phys. Lett. B **288**, 342 (1992).

[5] Y. Shamir, Nucl.Phys. B **406** 90 (1993); V. Furman and Y. Shamir, Nucl. Phys. B **439**, 54 (1995).

[6] P. H. Ginsparg and K. G. Wilson, Phys. Rev. D **25**, 2649 (1982).

[7] N. Neuberger, Phys. Lett. B **427**, 353 (1998).

[8] J. B. Kogut and L. Susskind, Phys. Rev. D **11**, 395 (1975).

[9] L. Susskind, Phys. Rev. D **16**, 3031 (1977).

[10] N. Kawamoto and J. Smit, Nucl. Phys. B **192** (1981) 100.

[11] H. S. Sharatchandra, H. J. Thun and P. Weisz, Nucl. Phys. B **192**, 205 (1981).

[12] M. F. L. Golterman and J. Smit, Nucl. Phys. B **245**, 61 (1984).

[13] L. H. Karsten, Phys. Lett. B **104**, 315 (1981).

[14] F. Wilczek, Phys. Rev. Lett. **59**, 2397 (1987).

[15] M. Creutz, JHEP 0804, 017 (2008) [arXiv:0712.1201 [hep-lat]].

[16] A. Borici, Phys. Rev. D **78**, 074504 (2008) [arXiv:0712.4401 [hep-lat]]; PoS LATTICE2008, (2008) [arXiv:0812.0092].

[17] M. Creutz, PoS LATTICE2008, (2008) [arXiv:0808.0014].

[18] M. Creutz and T. Misumi, Phys. Rev. D **82**, 074502 (2010) [arXiv:1007.3328];

[19] P. F. Bedaque, M. I. Buchoff, B. C. Tiburzi and A. Walker-Loud, Phys. Lett. B **662**, 449 (2008) [arXiv:0801.3361 [hep-lat]]; M. I. Buchoff, PoS LATTICE2008 (2008) [arXiv:0809.3943].

[20] P. F. Bedaque, M. I. Buchoff, B. C. Tiburzi and A. Walker-Loud, Phys. Rev. D **78**, 017502 (2008) [arXiv:0804.1145 [hep-lat]].

[21] T. Kimura and T. Misumi, Prog. Theor. Phys. **124**, 415 (2010) [arXiv:0907.1371 [hep-lat]].

[22] T. Kimura and T. Misumi, Prog. Theor. Phys. **123**, 63 (2010) [arXiv:0907.3774 [hep-lat]].

[23] K. Cichy, J. Gonzalez Lopez, K. Jansen, A. Kujawa and A. Shindler, Nucl. Phys. B **800**, 94 (2008) [arXiv:0802.3637 [hep-lat]].

[24] S. Capitani, J. Weber, H. Wittig, Phys. Lett. B **681**, 105 (2009) [arXiv:0907.2825].

[25] S. Capitani, J. Weber, H. Wittig, (2009) [arXiv:0910.2597].

[26] S. Capitani, M. Creutz, J. Weber, H. Wittig, JHEP 1009, 027 (2010) [arXiv:1006.2009].

[27] S. Aoki, Phys. Rev. D **30**, 2653 (1984).

[28] S. Aoki, Phys. Rev. D **33**, 2377 (1986); **34**, 3170 (1986); Phys. Rev. Lett. **57** 3136 (1986); Nucl. Phys. B **314**, 79 (1989).

[29] S. Sharpe and R. Singleton, Phys. Rev. D **58**, 074501 (1998).

[30] M. Creutz, (1996) [arXiv:hep-lat/9608024].

[31] V. Azcoiti, G. Di Carlo, A. Vaquero, Phys. Rev. D **79**, 014509 (2009); S. Sharpe, Phys.Rev. D **79**, 054503 (2009).

[32] M. Creutz, T. Kimura and T. Misumi, JHEP 1012, 041 (2010) [arXiv:1011.0761].

[33] B. Tiburzi, Phys. Rev. D **82** 034511 (2010).

[34] L. B. Drissi, E. H. Saidi, M. Bousmina, J. Math. Phys. **52** 022306 (2010).

[35] L. B. Drissi, E. H. Saidi, Phys. Rev. D **84** 014509 (2011).

[36] D. Chakrabarti, S. ands, A. Rago, JHEP 0906, 060 (2009).

[37] P. Hasenfratz, F. Karsch, Phys. Lett. B **125**, 308 (1983).

[38] T. Kimura, S. Komatsu, T. Misumi, T. Noumi, S. Torii and S. Aoki, JHEP **1201**, 048 (2012) [arXiv:1111.0402].

[39] J. M. Blairon, R. Brout, F. Englert and J. Greensite, Nucl. Phys. B **180** 439 (1981).

[40] D. J. Gross and A. Neveu, Phys. Rev. D **10**, 3235 (1974).

[41] T. Eguchi and R. Nakayama, Phys. Lett. B **126**, 89 (1983).

[42] S. Aoki and K. Higashijima, Prog. Theor. Phys. **76**, 521 (1986).

[43] B. Leder, Ph.D. Thesis, [arXiv:0707.1939].

[44] T. Korzec, Ph.D. Thesis, http://edoc.hu-berlin.de/docviews/abstract.php?id=28045 .

[45] B. Leder, JHEP 0804, 044 (2008) [arXiv:0711.1072].

[46] T. Izubuchi, J. Noaki and A. Ukawa, Phys. Rev. D **58**, 114507 (1998) [arXiv:hep-lat/9805019].

[47] T. Izubuchi and K. Nagai, Phys.Rev. D**61**, 094501 (2000) [arXiv:hep-lat/9906017].

[48] M. Creutz, T. Kimura and T. Misumi, Phys. Rev. D **83**, 094506 (2011) [arXiv:1101.4239].

[49] S. Kamata, H. Tanaka, [arXiv:1111.4536] (2011).

[50] H. Leutwyler, Phys. Rev. D **49**, 3033 (1994).

[51] T. Misumi, T. Kimura, A. Ohnishi, [arXiv:1206.1977] (2012).

[52] These two species are not equivalent since the gamma matrices are differently defined between them as $\gamma'_\mu = \Gamma^{-1}\gamma_\mu\Gamma$. In the above case it is given by $\Gamma = i\gamma_4\gamma_5$. This means the chiral symmetry possessed by this action is identified as a flavored one given by $\gamma_5 \otimes \tau_3$.